

Exploiting Magnetism and Magnetocaloric Effect in $\text{Nd}_{0.55}\text{Sr}_{0.45}\text{Mn}_{0.98}\text{Ga}_{0.02}\text{O}_3$

Bo Yu¹ · Hui Han² · Xiufeng Lan¹ · Weichun Zhang¹ · Lei Zhang² · Jiyu Fan¹

Received: 2 January 2017 / Accepted: 25 February 2017 / Published online: 7 March 2017
© Springer Science+Business Media New York 2017

Abstract We report results of the magnetization and magnetocaloric effect in lightly Ga-doped perovskite manganites $\text{Nd}_{0.55}\text{Sr}_{0.45}\text{Mn}_{0.98}\text{Ga}_{0.02}\text{O}_3$. It undergoes a second-order paramagnetic to ferromagnetic transition at $T_C = 250$ K and shows a strong ferromagnetic properties below T_C . However, an obvious upward deviation from the Curie-Weiss law far above T_C indicates the existence of non-Griffiths-like behavior in paramagnetic phase. Together with the measurements of isothermal magnetization around the Curie temperature, the unsaturated magnetization curves under high magnetic field of 7.0 T imply that the Ga-substitution causes the formation of antiferromagnetic phase due to some localized charge order phases generated in this composition. Based on the data of isothermal magnetization measured around T_C and Maxwell relation, we have calculated the maximum isothermal magnetic entropy change of 6.23 J/kg K for $\Delta\mu_0H = 7.0$ T magnetic field variation. Though only a moderate magnetic entropy change were obtained, a considerable large relative cooling power of 260 J/kg for $\Delta\mu_0H = 7.0$ T and 182 J/kg for $\Delta\mu_0H = 5.0$ T were found in this sample, this ensure it to be a potential candidate material to be applied in the magnetic refrigeration.

Keywords Manganite · Magnetocaloric effect · Phase transitions

1 Introduction

Perovskite manganites with the general formula $\text{A}_{1-x}\text{B}_x\text{MnO}_3$ (A = rare earth element, B = divalent alkaline earth element) are perceived as interesting materials with strong correlation between charge and spin degrees of freedom [1–4]. Extensive efforts to understand these mechanism have shown that the doping concentration x controls the band filling and the e_g electron transfer. The stoichiometric LaMnO_3 is an antiferromagnetic (AFM) insulator with A-type antiferromagnetism. By partial substitution with divalent elements B for La, a corresponding amount of Mn^{3+} was converted into Mn^{4+} , leading to the appearance of mixed-valence state $\text{Mn}^{3+}/\text{Mn}^{4+}$. Many studies have indicated that the double-exchange (DE) interaction between Mn^{3+} and Mn^{4+} can cause a strong paramagnetic-ferromagnetic (PM-FM) transition together with an insulator-metal (IM) transition around the Curie temperature. Therefore, the double exchange interaction together with electron-lattice coupling theories were proposed to understand the correlation between magnetic properties and electronic transport [5–7]. More recently, a viewpoint of the electronic/magnetic phase separation due to the intrinsically inhomogeneous and quenched disorder proposed by Dagotto et al. were used to explain the PM-FM phase transition together with IM transition in perovskite manganites [8]. Except for the intense investigations on fundamental physical properties, research in manganites has been also flourished since the finding of higher magnetic entropy change on these materials that provide potential application in magnetic refrigeration

✉ Jiyu Fan
jiyufan@nuaa.edu.cn

¹ Department of Applied Physics, Nanjing University of Aeronautics and Astronautics, Nanjing 210016, China

² High Magnetic Field Laboratory, Chinese Academy of Sciences, Hefei 230031, China

[9–12]. Such refrigeration is based on magnetocaloric effect (MCE) and viewed as environmentally friendly and energy efficient in solid state cooling technology compared with conventional vapor compression approach.

MCE is defined as an isothermal magnetic entropy change (MEC) as the magnetic material is exposed to a varying magnetic field. When an external field is applied, the atomic spin moments of magnetic materials are aligned parallel to the field which lowers the entropy and causes the sample to heat up. On the contrary, when the applied external field is removed, the spin tends to become random which increases the entropy and the material cools down. In general, there are two key factors for a magnetic material to be regarded as a good refrigerant, namely, a high concentration of magnetic moment and a strong temperature and field dependence of magnetization. Perovskite manganites can serve as excellent candidates for magnetic refrigeration applications because it just possess such two features.

The focus of this present paper is to study the magnetic properties and MCE of $\text{Nd}_{0.55}\text{Sr}_{0.45}\text{Mn}_{0.98}\text{Ga}_{0.02}\text{O}_3$ (NSMGO) compound. As we know, the ground state of half-doping manganites $\text{Nd}_{0.5}\text{Sr}_{0.5}\text{MnO}_3$ is a typical charge ordering AFM material while $\text{Nd}_{0.55}\text{Sr}_{0.45}\text{MnO}_3$ is FM material [13, 14]. The spatial CO phase, which can quite easily be observed in half-doped manganites $\text{R}_{0.5}\text{A}_{0.5}\text{MnO}_3$ ($\text{R} = \text{La, Pr, Nd}$; $\text{A} = \text{Sr, Ca}$) [15–19], behaves as the periodic arrangement of $\text{Mn}^{3+}/\text{Mn}^{4+}$ ions. Generally, the CO formation is accompanied by an AFM phase transition. Here, the latter composition is very close to the former. Therefore, when the Mn^{3+} ions of the latter is replaced with a slight other tervalence ions (such as Ga^{3+}), the ionic ratio of $\text{Mn}^{3+}:\text{Mn}^{4+}$ approaches to that of $\text{Nd}_{0.5}\text{Sr}_{0.5}\text{MnO}_3$. Thus, the system possibly generates some short-ranged CO AFM phases which coexist with the major FM phases. When an external field is applied on such a material with multiphase coexistence, it maybe induces some abnormal behaviors or a large MCE. Our results indicate that this sample shows an obvious characteristic of non-Griffith phase far above the Curie temperature even though it produces a drastic PM-FM phase transition at 250 K. Based on the measurements of temperature and field dependence of magnetization, we find that the localized CO phases not only exist in the system but also survive in the intensive FM background and form short-rang AFM correlations until to the lower temperature. According to the MEC scaling method, the PM-FM phase transition occurs at 250 K is confirmed to be second order. The maximum MEC and the highest relative cooling power (RCP) under magnetic field variation of 7.0 T are found to be 6.04 J/kg K and 260 J/kg around T_C , respectively. These results underline that our material can be also considered as a relevant potential candidate material to be used in cooling system based on the magnetic refrigeration.

2 Experiment

A polycrystalline NSMGO sample was prepared by traditional solid state reaction method. The structure and phase purity of the sample were checked by powder X-ray diffraction (XRD) using $\text{Cu K}\alpha$ radiation at room temperature. The XRD patterns prove that the sample is pure and a single-phase with orthorhombic structure. The magnetization versus temperature and magnetization versus magnetic field were measured by using a magnetic property measurement system (Quantum Design MPMS 7T-XL) with a superconducting quantum interference device (SQUID) magnetometer.

3 Results and Discussion

The XRD patterns at room temperature for the NSMGO sample is shown in Fig. 1. It is evidence that the sample shows typical reflections of the perovskite structure with orthorhombic symmetry. The structural parameters are refined by Rietveld's profile-fitting technique. The obtained results reveal that the diffraction data using the Rietveld powder diffraction profile fitting technique with space group Pnma give the lattice a , b , and c , of 5.477(1), 5.435(2), and 7.658(2). Obviously, the doping Ga^{3+} ions have partly replaced Mn^{3+} ions and occupied on B-site in the ABO_3 structure according to our design.

Figure 2 shows the temperature dependence of magnetization (M - T) of NSMGO measured under the magnetic field of 500 Oe. All data were measured on the warming process after zero-field cooling (ZFC, open sign) and field cooling (FC, solid sign), respectively. The M - T curve exhibits a sharp PM-FM phase transition. The Curie temperature (T_C), defined by the minimum in dM/dT , has been determined to be 250 K (see the inset of Fig. 2). To get a clear knowledge

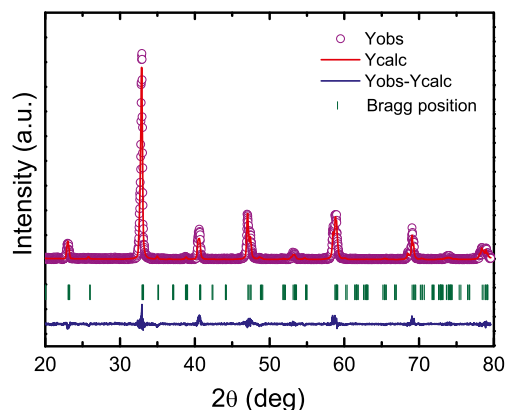


Fig. 1 Powder XRD patterns for $\text{Nd}_{0.55}\text{Sr}_{0.45}\text{Mn}_{0.98}\text{Ga}_{0.02}\text{O}_3$. Circles: experimental data. Red line: calculated pattern. Olive ticks: positions of the Bragg reflections for the main phase. Blue line: difference between the experimental and calculated patterns

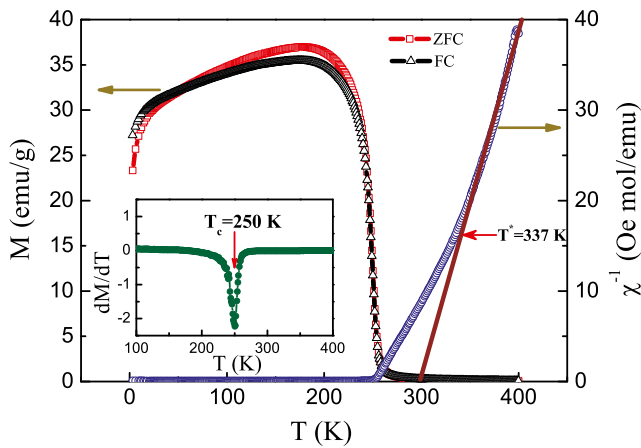


Fig. 2 The temperature dependence of magnetization measured at $H = 500$ Oe (left-hand axis) and the inverse magnetic susceptibility (right-hand axis). The solid lines represent the fitting data according to the Curie-Weiss law. Inset shows the first-order derivation of magnetization for temperature

about the magnetic interaction, the inverse magnetic susceptibility $1/\chi$ versus temperature has been also plotted in Fig. 2 (right-hand axis). For a ferromagnet, it is well known that in the PM region, the relation between χ and T , should follow the Curie-Weiss law, i.e., $\chi = \frac{C}{T-T_\theta}$, where T_θ is the Curie-Weiss temperature and C is the Curie constant. The positive value of T_θ fitted from the Curie-Weiss law confirms the existence of FM exchange interaction in this sample. With the obtained Curie constant C , the effective PM moment ($\mu_{eff} = 2.83\sqrt{C}\mu_B$) can be calculated to be $4.717 \mu_B$, which is a little bit larger than the calculated value $4.338 \mu_B$ using the spin-only moment of the free Mn ions (3.87 and $4.90 \mu_B$ for Mn^{4+} and Mn^{3+} , respectively). This result implies that the local FM coupling has possibly generated above the temperature of PM-FM phase transition.

It is worthy noting that there are an important feature occurred in the inverse magnetic susceptibility $1/\chi(T)$ curve. As the decrease of temperature, the $1/\chi$ versus T curve starts to deviate from the Curie-Weiss law and exhibits an upward departure from the linear dependence. The onset temperature of the deviation is denoted as T^* and it is around 337 K. Although the deviation from the Curie-Weiss law far above T_C which generally is considered to form well-known Griffiths phase is a common phenomenon for perovskite manganites in PM regime, it always shows as a downward deviation occurred in $1/\chi$ curve rather than an upturn deviation observed in this NSMGO sample. In most cases, the formation or existence of nanoscale ferromagnetic clusters well above PM-FM phase transition point usually cause the appearance of Griffiths phase where the short-range FM correlations in PM background change into long-range FM ordered state as the temperature decreases to T_C . Therefore, this behavior can be also understood and explained

with the viewpoint of phase separation. Here, what reason causes the abnormal upturn deviation? Note that the undoped $Nd_{0.55}Sr_{0.45}MnO_3$ system just lies at the boundary of ferromagnetic and charge order-antiferromagnetic (CO-AFM) phase. With the substitution of 2% Ga^{3+} for Mn^{3+} ions, it not only breaks the $Mn^{3+}-O^{2-}-Mn^{4+}$ magnetic order structures but also can cause considerable ionic disorder on Mn site. Under this circumstances, it is possible to form some short-range CO phases in some localized regions where the concentration ratio of $Mn^{3+}:Mn^{4+}$ is close to 1:1. Thus, the formation of some short-range AFM phases causes the decrease of total magnetization so that an upturn deviation from $1/\chi(T)$ curve is observed in Fig. 2. In fact, the similar phenomenon have been also observed in perovskite cobaltite $La_{1-x}Sr_xCoO_3$ and antiperovskite $Cu_{1-x}NMn_{3+x}$ [20, 21]. Both of them have testified that the existed short-range AFM state is the main reason for the observed upturn deviation from $1/\chi(T)$ curve.

Since a sharp PM-FM transition occurs around 250 K, which possibly implies a large MEC around T_C , we performed an investigation of MCE of the present material. In order to evaluate the MEC in this sample, as shown in Fig. 3, a series of isothermal magnetization curves from 230 to 270 K were measured with temperature interval 2.0 K. Obviously, all isothermal magnetization curves do not exhibit the sign of saturation even as the applied magnetic field reaches 7.0 T, further indicating the existence of CO AFM phase. The MCE which is an inherent property of a magnetic material is its response to the application or removal of magnetic field. Such response is maximized when the temperature is near the Curie temperature T_C . The total entropy can be defined as the sum of the entropy due to the lattice (S_L), the electrons (S_E), and the magnetic order (S_M). Under a constant pressure, this would be a function of both temperature and applied magnetic field. For an adiabatic processing, the application of a magnetic field leads to the decrease of S_E , then to the enhancement of S_L and,

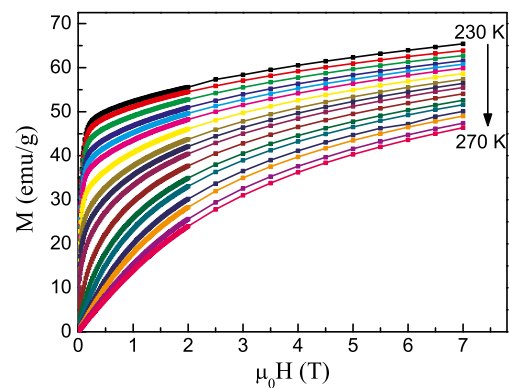


Fig. 3 Isothermal magnetization vs. magnetic field at different temperatures for $Nd_{0.55}Sr_{0.45}Mn_{0.98}Ga_{0.02}O_3$

therefore to the heating of the material. By analogy, the suppression of the magnetic field causes the cooling of the material. According to the classical thermodynamical theory, the isothermal MEC ΔS_M as a function of temperature and magnetic field can be calculated with Maxwell relation as follows

$$\begin{aligned}\Delta S_M(T, H) &= S_M(T, H) - S_M(T, 0) \\ &= \int_0^H \left(\frac{\partial M(T, H)}{\partial T} \right) \mu_0 dH\end{aligned}\quad (1)$$

In practice, the MEC $|\Delta S_M|$ can be evaluated from the isothermal magnetization measured with small temperature intervals, where $\Delta S_M(T, H)$ can be approximated as

$$|\Delta S_M| = \sum \frac{M_i - M_{i+1}}{T_{i+1} - T_i} \mu_0 \Delta H_i \quad (2)$$

where M_i and M_{i+1} are the experimental data of magnetization at T_i and T_{i+1} , respectively, under magnetic field $\mu_0 H_i$. It is normally expected that any material should have the largest MEC when its magnetization changes rapidly with temperature, i.e., in the vicinity of the magnetic phase transition temperature T_C . By using the above equation, the MEC vs temperature under different magnetic fields are presented in Fig. 4. As expected from Eq. 1, the MEC dependence on the temperature grows up to maximum values and increase with applied magnetic field. For a field change of $\Delta\mu_0 H = 7.0$ T, the maximum MEC ΔS_M is about 6.23 J/kg K. The MCE in the perovskite manganites mainly originates from the spin lattice coupling related to the magnetic ordering process. The strong coupling between the spin and lattice is shown by the observed lattice changes accompanying magnetic transitions in these manganites. The lattice structural change in the Mn-O bond distances and Mn-O-Mn bond angles with temperature, which exhibit variation in the volume, can cause an additional change in magnetism. Although a few intermetallic compounds, viz.,

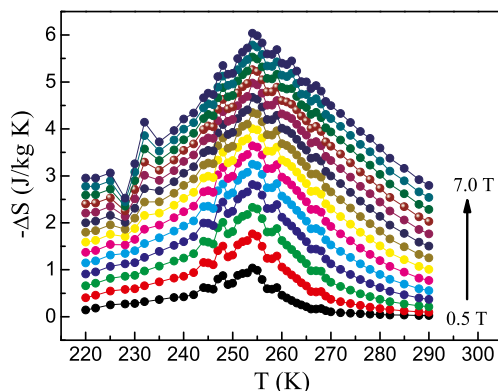


Fig. 4 Magnetic entropy change (ΔS_M) plotted as a function of temperature at different applied fields

some members of the Heusler alloys [22, 23], Laves phase [24, 25], etc. are known to exhibit even larger MCE, the value of MEC obtained in NSMGO sample is large enough to be used in magnetic refrigeration.

On the other hand, RCP is another important parameter to determine the cooling efficiency of magnetic refrigerants and evaluated through the amount of heat transferred between the cold and hot sinks in the ideal refrigeration cycle. RCP is generally calculated by integrating the $(\Delta S_M - T)$ curves over the full width at half maximum using the relation $RCP = \int_{T_{cold}}^{T_{hot}} \Delta S_M dT$. Generally, RCP can be approximately estimated with $RCP \cong \Delta S_{Mmax} \delta T_{FWHM}$, where δT_{FWHM} is the full width at half maximum of magnetic entropy change curve. The data of RCP under different magnetic fields can be calculated according to the inset of Fig. 5. As shown in Fig. 5, the obtained RCP values increase with the applied magnetic field indicating that RCP is strong field dependent. The largest RCP is found to be 260 J/kg for 7.0 T magnetic field change and 182 J/kg for 5.0 T magnetic field change which is very large compared to other perovskite manganites and it is of 44.3% that of pure Gd for $\Delta\mu_0 H = 5.0$ T [26]. Therefore, our NSMGO material can be considered as a potential candidate material to be applied in the magnetic refrigeration.

Recently, Franco et al. have proposed a useful fundamental method to construct the universal curve based on the MEC that can be used to access the nature of phase transitions for a wide range of magnetic materials [27]. Based on the scaling relation, they suggested a phenomenological universal scaling of $\Delta S_M(T, H)$ in which if the magnetization of single-phase materials exhibiting the second-order phase transition is measured at different applied fields and temperatures, their $\Delta S_M(T, H)$ curves can collapse into a single

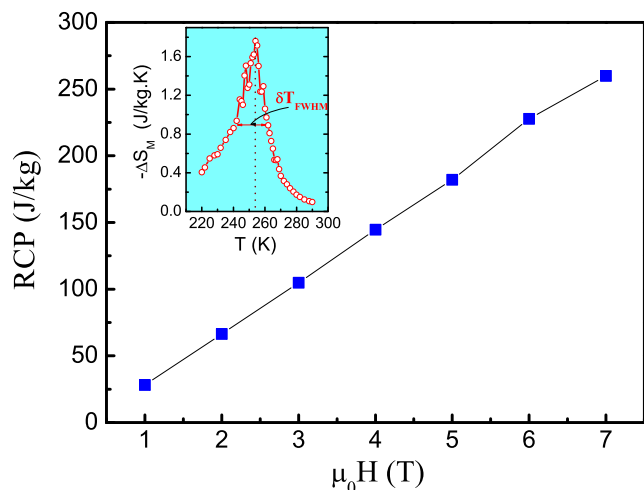


Fig. 5 The value of RCP as a function of magnetic field. The inset shows $-\Delta S_M$ vs. T curve at $\mu_0 H = 1.0$ T, the line with double arrows represents the full width at half maximum of magnetic entropy change

curve. Therefore, the order of phase transition in the present system should be further clarified by utilizing this method. The detailed treatment solution can be performed according to the following protocol. First, two points are selected from each ΔS_M vs. T curves (Fig. 4). One (T_{r1}) is below T_{peak} and the other (T_{r2}) is above T_{peak} . Both of them should satisfy the relation $\Delta S_M(T_{r1}) = \Delta S_M(T_{r2}) = k\Delta S_M^{peak}(T_{peak})$, where ΔS_M^{peak} is the maximum value of the selected ΔS_M vs. T curves and k is the relative value of the entropy changes at two reference temperatures T_{r1} and T_{r2} . Generally, the selection of k value is arbitrary but k value is always between 0 and 1. Here, we choose the $k=0.7$ to construct the “universal master curve”. Two reference temperatures are used here and the temperature axis is rescaled as:

$$\theta = \begin{cases} \theta_- = (T_{peak} - T)/(T_{r1} - T_{peak}), & T < T_{peak} \\ \theta_+ = (T - T_{peak})/(T_{r2} - T_{peak}), & T > T_{peak} \end{cases} \quad (3)$$

As shown in Fig. 6, all the ΔS_M vs. T curves under different magnetic fields collapse into a single curve. Therefore, the PM-FM phase transition in NSMGO material was confirmed to be second order.

Based on the obtained MEC and non-Griffith behavior observed from the inverse magnetic susceptibility $1/\chi(T)$ curve, we can propose the following scenario for completely understanding the whole magnetism and magnetic phase transition in NSMGO. For the pristine $\text{Nd}_{0.55}\text{Sr}_{0.45}\text{MnO}_3$, it generates the long-range FM coupling through the double exchange interaction by the $\text{Mn}^{3+}\text{-O}^{2-}\text{-Mn}^{4+}$ spin chain. As the partial Mn^{3+} ions are replaced by Ga^{3+} ions, they not only randomly occupy B-site sublattice and generate a certain kind of chemical disorder in the system, but also make the ratio of $\text{Mn}^{3+}:\text{Mn}^{4+}$ to approach the typical CO system of 1:1. Therefore, in some localized regions, the formation

of short range CO-AFM phases are feasible. In fact, from the unsaturated isothermal magnetization curves of Fig. 3 and the reduction of magnetization in lower temperature of Fig. 2, we are convinced that these CO phases definitely exist in the system. On the other hand, we also noticed that the CO phases undoubtedly influenced and played some roles in the MEC. In Fig. 4, as the $\Delta\mu_0H \leq 4.0$ T, we can only observed one peak and one maximum MEC on $\Delta S_M(T,H)$ curves. However, as the $\Delta\mu_0H > 4.0$ T, the second peak occurs around 235 K. Although we unable to give a definite conclusion that this new peak positively originates from the localized CO AFM transition under high magnetic field, both of them must have some relations. The temperature of $T = 235$ K is far below $T_C = 250$ K, where the system has entered into FM state. Whatever the residual PM phases or some FM clusters, they are impossible to generate magnetic phase transition only under the enough high magnetic fields. Moreover, from the rescaling $\Delta S_M(T,H)$ curves, we can find that, except for the region around $T = 235$ K, the other parts all show good normalization feature. It implies that the transition at 235 K could be one-order phase transition instead of second-order. In fact, many previous works have testified that the CO AFM phase transition belongs to one-order [28, 29]. Here, the detailed analysis and investigation of the short-range CO AFM phase in NSMGO sample have been beyond the scope of this paper. The better method for this issue need more experimental measurements on high purity single crystalline sample in the future works.

4 Conclusion

In summary, we have reported the magnetic properties and MEC of the perovskite manganite $\text{Nd}_{0.55}\text{Sr}_{0.45}\text{Mn}_{0.98}\text{Ga}_{0.02}\text{O}_3$. The temperature and magnetic field dependence on magnetization measurements combined suggest that the localized CO AFM phases generate in PM state and can survive in strong FM background as the temperature decreases to the lowest temperature. A sharp PM-FM phase transition occurred in T_C decides a noticeable MEC and a large RCP in this sample making it to be considered as a potential candidate material to be applied in the magnetic refrigeration. Together with the the rescaling analysis performed on $\Delta S_M(T,H)$ curves, the observed PM-FM phase transition has been verified to be second-order. Nevertheless, another peak of MEC and unnormalized $\Delta S_M(T,H)$ curves at 235 K also indicate that there are one-order phase transition driven by applied magnetic field in NSMGO sample.

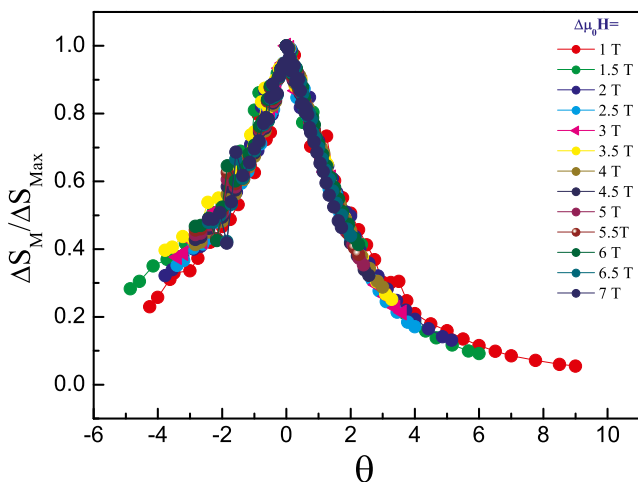


Fig. 6 Normalized magnetic entropy change dependence on the rescaled temperatures

Acknowledgment This work was supported by the National Nature Science Foundation of China (Grant nos. 11574322 and U1332140) and the Foundation for Users with Potential of Hefei Science Center (CAS) through Grant No. 2015HSC-UP001.

References

1. von Helmolt, R., Wecker, J., Holzapfel, B., Schultz, L., Samwer, K.: Giant negative magnetoresistance in perovskitelike $\text{La}_{2/3}\text{Ba}_{1/3}\text{MnO}_x$ ferromagnetic films. *Phys. Rev. Lett.* **71**, 2331 (1993)
2. Jin, S., Tiefel, T.H., McCormack, M., Fastnacht, R.A., Ramesh, R., Chen, L.H.: Thousandfold Change in Resistivity in Magnetoresistive La-Ca-Mn-O Films. *Science* **264**, 413 (1994)
3. Mori, S., Chen, C.H., Cheong, S.-W.: Paired and Unpaired Charge Stripes in the Ferromagnetic Phase of $\text{La}_{0.5}\text{Ca}_{0.5}\text{MnO}_3$. *Phys. Rev. Lett.* **81**, 3972 (1998)
4. Yunoki, S., Hu, J., Malvezzi, A.L., Moreo, A., Furukawa, N., Dagotto, E.: Phase Separation in Electronic Models for Manganites. *Phys. Rev. Lett.* **80**, 845 (1998)
5. Zener, C.: Interaction between the d shells in the transition metals. *Phys. Rev.* **82**, 403 (1951)
6. Millis, A.J., Littlewood, P.B., Shraiman, B.I.: Double exchange alone does not explain the resistivity of $\text{La}_{1-x}\text{Sr}_x\text{MnO}_3$. *Phys. Rev. Lett.* **74**, 5144 (1995)
7. De Teresa, J.M., Ibarra, M.R., Algarabel, P.A., Ritter, C., Marquina, C., Blasco, J., Garcia, J., del Moral, A., Arnold, Z.: Evidence for magnetic polarons in the magnetoresistive perovskites. *Nature(London)* **386**, 256 (1997)
8. Dagotto, E., Hotta, T., Moreo, A.: Colossal magnetoresistant materials: the key role of phase separation. *Phys. Rep.* **344**, 1 (2001)
9. Phana, M.-H., Yu, S.-C.: Review of the magnetocaloric effect in manganite materials. *J. Magn. Magn. Mater.* **308**, 325 (2007)
10. Naik, V.B., Barik, S.K., Mahendiran, R., Raveau, B.: Magnetic and calorimetric investigations of inverse magnetocaloric effect in $\text{Pr}_{0.46}\text{Sr}_{0.54}\text{MnO}_3$. *Appl. Phys. Lett.* **98**, 112506 (2011)
11. Rostamnejadi, A., Venkatesan, M., Kameli, P., Salamati, H., Coey, J.M.D.: Magnetocaloric effect in $\text{La}_{0.67}\text{Sr}_{0.33}\text{MnO}_3$ manganite above room temperature. *J. Magn. Magn. Mater.* **323**, 2214 (2011)
12. Zhang, Y., Lampen, P.J., Phan, T.-L., Yu, S.-C., Srikanth, H., Phan, M.-H.: Tunable magnetocaloric effect near room temperature in $\text{La}_{0.7-x}\text{Pr}_x\text{Sr}_{0.3}\text{MnO}_3$ ($0.02 \leq x \leq 0.30$) manganites. *J. Appl. Phys.* **111**, 063918 (2012)
13. Kawano-Furukawa, H., Kajimoto, R., Yoshizawa, H., Tomioka, Y., Kuwahara, H., Tokura, Y.: Orbital order and a canted phase in the paramagnetic and ferromagnetic states of 50% hole-doped colossal magnetoresistance manganites. *Phys. Rev. B* **68**, 174422 (2003)
14. Xu, L., Fan, J., Shi, Y., Zhu, Y., Bärner, K., Yang, C., Shi, D.: Critical behavior and long-range ferromagnetic order in perovskite manganite $\text{Nd}_{0.55}\text{Sr}_{0.45}\text{MnO}_3$. *EPL* **112**, 17005 (2015)
15. Rao, C.N.R., Cheetham, A.K.: Materials science-Charge Ordering In Manganates. *Science* **276**, 911 (1999)
16. Tokura, Y., Nagaosa, N.: Orbital physics in transition-metal oxides. *Science* **288**, 462 (2000)
17. Schiffer, P., Ramirez, A.P., Bao, W., Cheong, S.W.: Low temperature magnetoresistance and the magnetic phase diagram of $\text{La}_{1-x}\text{Ca}_x\text{MnO}_3$. *Phys. Rev. Lett.* **75**, 3336 (1995)
18. Tomioka, Y., Asamitsu, A., Moritomo, Y., Kuwahara, H., Tokura, Y.: Collapse of a charge-ordered state under a magnetic field in $\text{Pr}_{1/2}\text{Sr}_{1/2}\text{MnO}_3$. *Phys. Rev. Lett.* **74**, 5108 (1995)
19. Kuwahara, H., Tomioka, Y., Asamitsu, A., Moritomo, Y., Tokura, Y.: A first-order phase transition induced by a magnetic field. *Science* **270**, 173 (1995)
20. He, C., Torija, M.A., Wu, J., Lynn, J.W., Zheng, H., Mitchell, J.F., Leighton, C.: Non-Griffiths-like clustered phase above the Curie temperature of the doped perovskite cobaltite $\text{La}_{1-x}\text{Sr}_x\text{CoO}_3$. *Phys. Rev. B* **76**, 014401 (2007)
21. Lin, J., Tong, P., Cui, D., Yang, C., Yang, J., Lin, S., Wang, B., Tong, W., Zhang, L., Zou, Y., Sun, Y.: Unusual ferromagnetic critical behavior owing to short-range antiferromagnetic correlations in antiperovskite $\text{Cu}_{1-x}\text{NMn}_{3+x}$ ($0.1 \leq x \leq 0.4$). *Sci. Rep.* **5**, 7933 (2015)
22. Liu, J., Gottschall, T., Skokov, K.P., Moore, J.D., Gutfleisch, O.: Giant magnetocaloric effect driven by structural transitions. *Nature Mater.* **11**, 620 (2012)
23. Franco, V., Blázquez, J.S., Ingale, B., Conde, A.: The magnetocaloric effect and magnetic refrigeration near room temperature: materials and models. *Annu. Rev. Mater. Res.* **42**, 305 (2012)
24. Shen, B.G., Sun, J.R., Hu, F.X., Zhang, H.W., Cheng, Z.H.: Recent progress in exploring magnetocaloric materials. *Adv. Mater.* **21**, 4545 (2009)
25. Singh, N.K., Kumar, P., Suresh, K.G., Nigam, A.K., Coelho, A.A., Gama, S.: Itinerant electron metamagnetism and magnetocaloric effect in RCO_2 -based Laves phase compounds. *J. Phys.: Condens. Matter* **19**, 036213 (2007)
26. Pecharsky, V.K., Gschneidner, K.A., Tsokol, A.O.: Recent developments in magnetocaloric materials. *Rep. Prog. Phys.* **68**, 1479 (2005)
27. Bonilla, C.M., Herrero-Albillos, J., Bartolome, F., Garcia, L.M., Parra-Borderias, M., Franco, V.: Universal behavior for magnetic entropy change in magnetocaloric materials: An analysis on the nature of phase transitions. *Phys. Rev. B* **81**, 224424 (2010)
28. Fan, J., Hong, B., Ying, Y., Ling, L., Pi, L., Zhang, Y.: Strain-driven inverse thermal hysteresis behaviour in half-doped manganites. *J. Phys. D: Appl. Phys.* **41**, 105013 (2008)
29. Phan, M.H., Morales, M.B., Bingham, N.S., Srikanth, H., Zhang, C.L., Cheong, S.W.: Phase coexistence and magnetocaloric effect in $\text{La}_{5/8-y}\text{Pr}_y\text{Ca}_{3/8}\text{MnO}_3$ ($y=0.275$). *Phys. Rev. B* **81**, 094413 (2010)